AJNR

Acute and Chronic Swine Rete Arteriovenous Malformation Models: Effect of Ethiodol and Glacial Acetic Acid on Penetration, Dispersion, and Injection Force of n-Butyl 2-Cyanoacrylate

B. B. Lieber, A. K. Wakhloo, R. Siekmann and M. J. Gounis

AJNR Am J Neuroradiol 2005, 26 (7) 1707-1714
http://www.ajnr.org/content/26/7/1707

AJNR Am J Neuroradiol 26:1707–1714, August 2005

Acute and Chronic Swine Rete Arteriovenous Malformation Models: Effect of Ethiodol and Glacial Acetic Acid on Penetration, Dispersion, and Injection Force of N-Butyl 2-Cyanoacrylate

B. B. Lieber, A. K. Wakhloo, R. Siekmann, and M. J. Gounis

BACKGROUND AND PURPOSE: **Liquid embolic agents are increasingly gaining importance in the embolization of cerebral arteriovenous malformations (AVMs). Currently, the most commonly used agent is N-butyl 2-cyanoacrylate (NBCA). Various NBCA mixtures, arterial hypotension, and Valsalva maneuver (increased positive end-expiratory pressure) during the injection of the acrylate have been used to address hemodynamic and architectural variations of an AVM; however, the precise in vivo polymerization, distribution, and kinetics of NBCA mixtures are unknown. We investigated the effect of different acrylate/Lipiodol mixtures and the addition of glacial acetic acid (GAA) on the penetration, dispersion, and injection force of NBCA.**

METHODS: **A swine rete AVM model that has been described elsewhere was used for the embolization. In one subgroup of animals, embolization was performed immediately after construction of the AVM model. In a second subgroup, a chronic AVM model was used. GAA was added to the NBCA mixture to decrease the pH value of the solution and prolong the polymerization time. The addition of GAA allowed us to reduce the amount of Lipiodol, thereby reducing the viscosity of the mixture.**

A total of 30 swine were used for both the acute ($n = 23$) and chronic ($n = 7$) subgroups. The following mixtures of Lipiodol/NBCA and GAA (% vol/%vol + μL) were used for embolization: 80/20 + 0; 50/50 + 0; 50/50 + 5; 50/50 + 10; and 50/50 + 20. A total of six retia per mixture were used for the analysis. Glue injection pressure profiles were recorded in each experiment. High-resolution radiographic images obtained from the harvested retia were used to correlate the dispersion and depth of glue penetration with the AVM hemodynamics. The effect of different amounts of GAA on the glue dispersion and depth of penetration of the mixtures was also studied.

RESULTS: **Using the same pressure gradients, less viscous NBCA + GAA mixtures led to a deeper nidal penetration. The addition of 20 μL of GAA resulted in a three times higher penetration and dispersion of the NBCA mixture that was more homogenous.**

CONCLUSION: **The viscosity of the liquid embolic agent used is an important limiting factor for an AVM embolization. Reducing the amount of Lipiodol improves nidus penetration. Quicker polymerization can be overcome by adding GAA, which reduces the pH of the mixture.**

Various embolic materials have been used with various degrees of success to embolize arteriovenous malformations; however, the use of cyanoacrylates, particularly N-butyl 2-cyanoacrylate (NBCA), as the embolic agent is frequently advocated (1–5). Although embolization alone has a limited value in the permanent successful obliteration of an AVM, it is considered a valid approach for patients having an AVM that cannot be treated by surgery or radiation. An AVM can be completely embolized if the embolic agent casts the entire AVM nidus. Proximal occlusion of the feeding arteries without deep glue penetration into the nidus usually results in revascularization and regrowth of the AVM (3, 6, 7). The embolic agent must reach the proximal end of the venous compartment adjacent to the AVM nidus, because collateralization in a partially occluded AVM may develop into the same initial draining veins (6). Conversely, oblit-

Received September 21, 2004; accepted after revision January 26.

From the Departments of Biomedical Engineering (B.B.L., A.K.W., M.J.G.) and Radiology (B.B.L., A.K.W.), University of Miami, Coral Gables, FL; and the Department of Neuroradiology (R.S.), University of Giessen, Giessen, Germany.

Address correspondence to B. Barry Lieber, Department of Biomedical Engineering, University of Miami, 1251 Memorial Drive, Coral Gables, FL 33146.

eration of the AVM draining vein(s) will result in increased intranidal pressure, which can augment the risk of swelling and hemorrhage (8). In addition, the penetration of embolic material into the venous channels may result in pulmonary complications (9).

To improve nidal acrylate embolization, we studied the dispersion of NBCA in both acute and chronic swine rete models simulating a plexiform human AVM (10). Iodized oil was added to NBCA to delay the polymerization time and angiographically visualize the dispersion and penetration of NBCA into the pathology. A variation in the mixing ratio of Lipiodol to NBCA was used in an attempt to delay the polymerization of the embolic mixture. We prepared mixtures of Lipiodol/NBCA that are commonly used in the clinical setting and examined the mixture's composition effect on the penetration and dispersion within the rete. We further investigated how reducing the pH of the mixture by adding GAA affected its dispersion.

Methods

AVM Model in Rete of Swine

A total of 49 barnyard and Yucatan swine of mixed sex were used in this study (37 acute AVM-rete models and 12 chronic models). Angiograms were obtained by using a digital subtraction angiography (DSA) unit (Toshiba TDA 4000; Toshiba Corporation, Otawara-Shi, Japan). The follow-up angiograms were documented at frame rates ranging from 3.75 to 7 frames per second, with images of 1024 × 1024 pixels and 4096 gray-scale resolution (image depth).

Acute AVM Model

The construction of the acute swine rete AVM model has been described previously by Siekmann et al (11). A large guide catheter was placed in the left common carotid artery with its distal tip wedged into the origin of the left ascending pharyngeal artery (APA). The proximal side (hub) of the catheter, now serving as a cannula, was opened to atmospheric pressure just before and during embolization. The cannula replaced the surgical procedure involved in creating the AV fistula and provided a sufficiently large pressure drop to establish retrograde flow through the cannulated side of the rete. A microcatheter (FasTracker 18, Boston Scientific/Target Therapeutics, Fremont, CA) was navigated through the guide catheter into the middle of the right APA. Superselective angiograms with and without opening the draining catheter to the atmospheric pressure were obtained to document the efficacy of the model. The acute model was then established and ready to use on demand when the cannula was opened.

The microcatheter was kept in the APA and flushed several times with a 5% dextrose solution to remove ion-containing contrast or saline. The glue mixture was prepared in a separate area and loaded into a 3-mL syringe for injection. A 3-mL syringe with an inner diameter of 8.66 mm was used instead of a 1-mL syringe, to eliminate the need for syringe exchange during glue injection and provide continuous injection of the glue. A total of 23 successful experiments were available for data analysis.

Chronic AVM Model

The prepared cranium was connected to an ex vivo mock circulation loop (10). The flow loop was perfused with 3–3.5 L of the animal blood containing ethylene diamine tetra-acetic acid (solution concentration 7.5%, 20 mL/L blood) to prevent coagulation. The blood was drawn from the animal via the femoral artery before sacrifice. During the experiment, blood was stirred continuously at 37°C by using a laboratory magnetic stirrer/hot plate (model PC-420; Corning Inc., Corning, NY). A peristaltic metering pump (Cole-Parmer Instrument Co., Chicago, IL) was used to circulate the blood.

Two shunts were built into the perfusion loop, which was constructed of Tygon tubes with .25-inch inner diameter. The first shunt consisted of a Starling resister that was adjusted to 170 mm Hg pressure to regulate the maximum pressure through the test section. A bypass valve acted as a second shunt to purge the air from the flow rig before connecting the test section.

The blood flow through the rete was measured in the return line by using an electromagnetic flow meter system (transducer model SP75519 and meter model SP2202; Gould Stantham, Oxnard, CA). Blood pressure at inlet and outlet was measured by using Deltran disposable pressure transducers (Utah Medical Products, Inc., Midvale, UT) with an operating range of −50 to 300 mm Hg. The transducers were connected to a bridge amplifier (Tri-Pack model TP8891, Vivitro System, Inc., Victoria, Canada). In addition, during embolization the injection pressure of the glue was recorded with a differential pressure measurement system (transducer model DP15–36 and digital transducer indicator model CD223; Validyne Engineering Corp., Northridge, CA).

Before each experiment, all the pressure transducers were calibrated by using a mercury-in-glass manometer and the flow transducer was calibrated by using a graduated cylinder and stopwatch. The signals from all four transducers (three pressure values, one flow) were recorded and stored on a personal computer for further off-line analysis.

The FasTracker18 microcatheter was placed into the APA leading to the rete, which represented the AVM nidus. Before each embolization, 5 mL of iodinated contrast material (Oxilan 300; Guerbet LLC, Bloomington, IN) was injected to obtain a digitally subtracted angiogram. The microcatheter was then flushed several times with a 5% dextrose solution to remove ion-containing saline and contrast. For the chronic experiments, 1-mL syringes with 4.78-mm inner diameter were used for embolization. The same senior investigator (A.K.W.) carried out a manual injection of the glue into the rete via the microcatheter. Real-time fluoroscopy was used to monitor the injection and document the acrylate distribution within the APA and the rete. In the chronic group, a total of 12 AVM models were created. Four served as model development experiments, and one experiment was excluded because of technical difficulties in harvesting the rete. Thus, seven successful experiments were used from a total of eight for further analysis. The average age of the animals at surgical creation of the AVM model was about 6 months, whereas the average age of the animals at embolization was about 12.4 months. The time elapse between model creation and embolization ranged between 6 and 7 months. The retia were harvested immediately following embolization and subjected to further analysis.

Radiograms and Histology

Control angiograms of the rete, while inside the cranium, were obtained after acrylate injection through the guide catheter. Thereafter, the rete was harvested and fixed in 10% formaldehyde solution for further histologic studies. Before paraffin embedment, high-resolution radiographic digital images (1024 × 1024 pixels with a resolution of 10–11 line pairs/mm) of the retia were obtained (Fig 1) by using a mammography unit working at a 0.1-mm micro–focal spot (Mammotest/Mammovision unit; Fisher Imaging Co., Denver, CO). The images were used to analyze the penetration depth and dispersion of the various mixtures, which were performed in defined hemodynamic conditions at the time of embolization. Image processing and mathematical modeling were applied to

FIG 1. Radiograms of a harvested embolized rete obtained from a mammography unit operating at a 0.1-mm micro–focal spot. The Lipiodol/NBCA+GAA mixture penetrated most of the rete (*arrow* indicates the direction of blood flow).

the data to analyze the dispersion of the various acrylate mixtures.

Analysis Methods

Image Processing and Data Reduction. The centerline of each rete was defined as the locus of the points obtained by a thinning operation (Fig 2). A sector scan algorithm was developed to quantify the summed grayscale value of each sector along the centerline of each rete. By demarcation of a midline, the rete was divided into right and left halves. The location of the midline was determined by vertical line scans, 1 pixel wide, of the rete in the vicinity of the midline to find the most slender location. A point on the midline of the rete (o) was defined as the origin of the coordinate system (Fig 3*A*). A polar coordinate system was applied to the rete above the origin, whereas below the origin a Cartesian coordinate system was applied. Below the origin, the cumulative grayscale values were calculated for segments of height ΔS and assigned to the center of the segment on the centerline (Fig 3*A*). Above the origin sectors of angle $\Delta\theta$ were used. The criteria for selecting the origin of the coordinate system on the midline were as follows. First, the angle of the sector, $\Delta\theta$, was selected such that $\bar{r}\,\Delta\theta = \Delta S$, where $\bar{r}$ is the average radius of the sector $\bar{r} = 0.5\,(r_1 + r_2)$. Second, an arc length of $\bar{\rho}\Delta\theta \geq 1$ pixel (where $\bar{\rho} = 0.5\,[\rho_1 + \rho_2]$) was imposed to avoid sector edge overlap inside the rete. The cumulative intensity levels of sectors along the centerline were normalized by the maximum value for that rete for further analysis. Figure 3*B* shows sectors in which cumulative grayscale values (or image intensity) are determined.

The rete was considered to begin at the first bifurcation of the APA and be symmetric around the origin. Therefore, the length of each rete was determined as twice the length of the centerline from the first bifurcation of the APA to the midline on the embolized side. Two scans were performed on each image. In the first scan, the cumulative grayscale values for the rete, including the embolized vasculature, were determined (Fig 4*A*). The second scan was performed after all structures other than the embolized vessels were removed from the image by threshold filtering (Fig 4*B*). The cumulative grayscale intensities of the scans (as fraction of maximum) before and after threshold filtering (Fig 5*A*) were used to construct the glue penetration function (Fig 5*B*) as the ratio of the aforementioned two variables shown in Fig 5*A*. Mathematical modeling was employed to obtain the penetration depth and the dispersion of various glue mixtures in the vasculature of the rete.

FIG 2. Centerline superimposed on the rete image.

Mathematical Modeling. A mathematical function consisting of four parameters (see Appendix) was developed to model the penetration depth and the dispersion of the embolic mixture in the rete. The four parameters of the function include the amplitude (A) of the glue penetration function, the penetration depth of the glue (l_g), the cumulative grayscale intensity of the rete at the maximum glue penetration depth (i_r), and the dimensionless dispersion parameter (D). The values of the parameters were obtained by a constrained optimization process (see Appendix) in which the error between the data and the prediction is minimized in a least-squares sense.

Evaluation and interpretation of the function amplitude and the glue penetration depth are straightforward. The dispersion parameter of the model, D, however, cannot be obtained directly, because the rete is not a monotonically distributing network of branches. Unlike a tree, where successive branching occurs from the trunk toward the outer margins of the crown, crossing the rete, from one APA to the other, a sharp increase in the number of vessels occurs, followed some reduction in the number of branches toward the midline followed by yet another increase past the midline and than a rapid decrease until all the vessels coalesce into the contralateral APA. Therefore, the exponential coefficient λ of equation (A1) needs to be evaluated first. Thereafter, the dispersion parameter can be obtained through the scaling of λ by a geometrically related parameter of the rete such as i_r (equation [A2]). Once λ and l_g

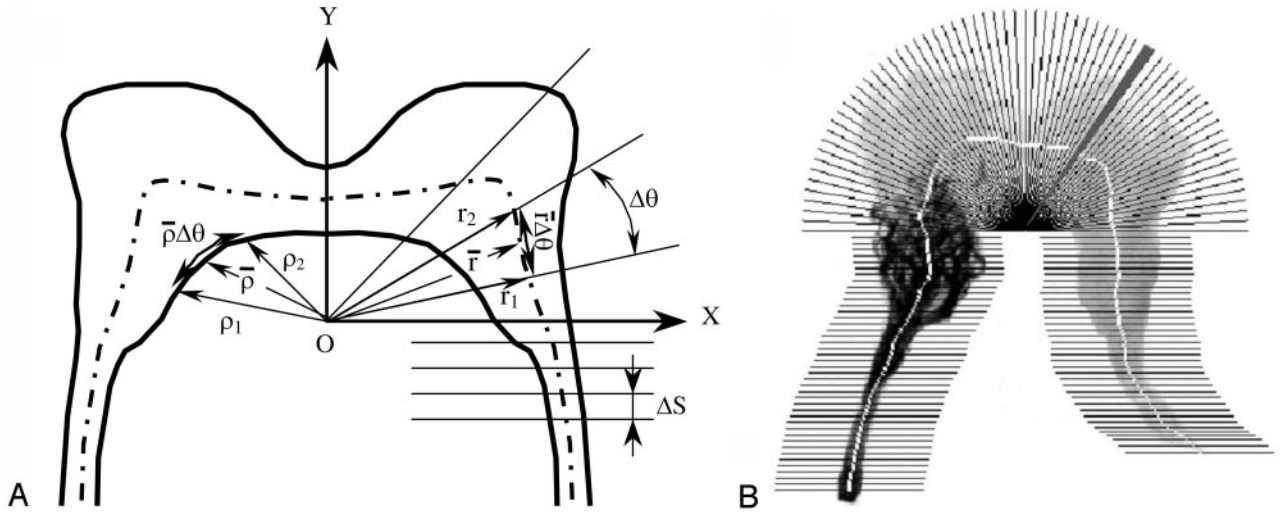

FIG 3. Quantification of the grayscale of a rete image with glue cast.
A, Determination of the rete coordinate system and the angular sampling rate.
B, Sectors along the centerline for calculations of the cumulative intensity values within each sector (one sector is shaded for presentation).

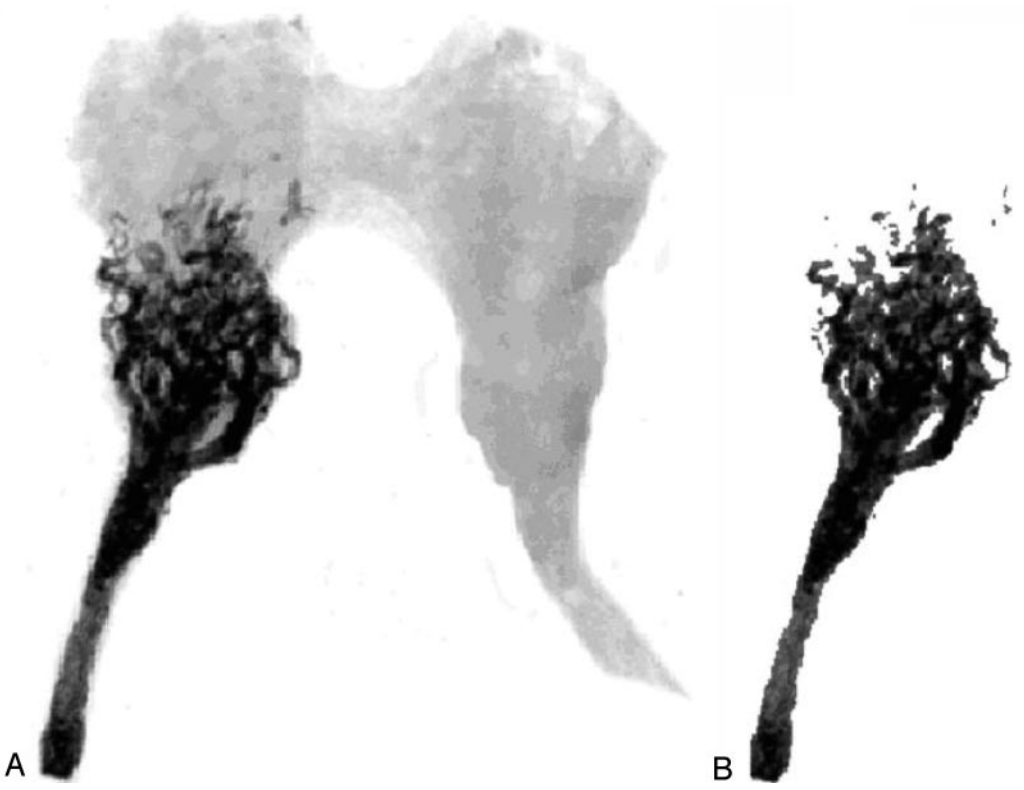

FIG 4. *A,* Radiograph of a rete embolized with 50/50 + 0 μL Lipiodol/NBCA+GAA. *B,* Image of embolized vessels only after threshold filtering.

have been evaluated by using equation A1, the dispersion parameter is determined from equation (A2), and the normalized penetration depth, *L,* is calculated by using equation (A7). The force and the impulse of glue injection are calculated from the measured injection pressure by using equation (A8).

Statistical Analysis. Statistical analyses were performed by using SPSS (SPSS, Inc., Chicago, IL), Instat (GraphPad Software, Inc., San Diego, CA), and Microsoft Excel (Microsoft, Inc., Redmond, WA). Penetration depths in each embolic mixture group were normalized by their respective mean rete length. An equivalent test was done to assess the effect of the Lipiodol concentration on the penetration depth and the dispersion parameter between 80/20 + 0 and 50/50 + 0 mixtures.

The means of penetration depths and dispersion parameters of the different glue mixtures were compared by using a one-way analysis of variance (ANOVA) test. ANOVA assumes that the data are sampled from populations that follow Gaussian distributions. This assumption was tested by using the Kolmogorov/Smirnov method. ANOVA also assumes that the data are sampled from populations with identical standard deviations (SDs). This second assumption was tested by using the Bartlett method. When the SDs were unequal, the means were com-

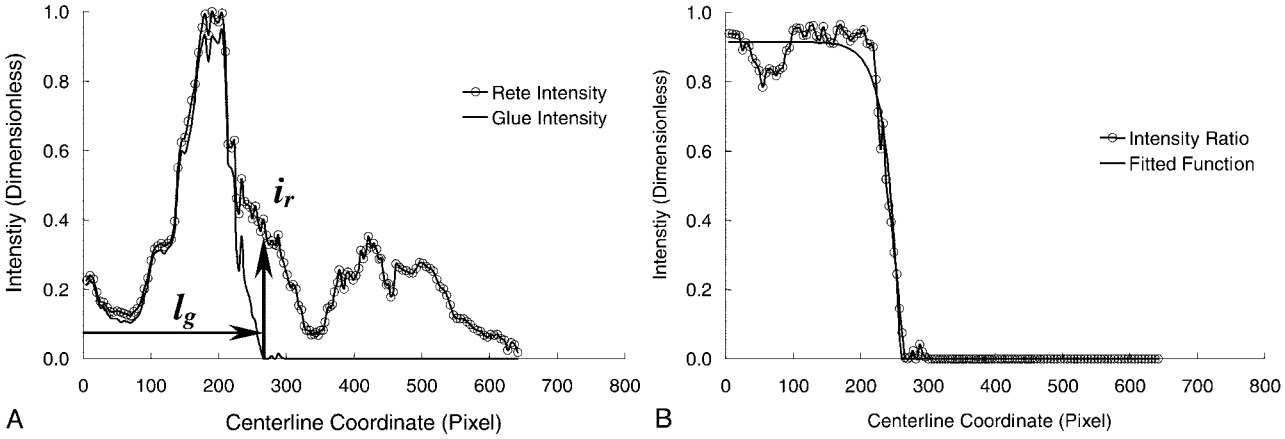

FIG 5. *A,* Sector averaged grayscale intensity profiles for the rete (of Fig 4), including the embolized vasculature and for only the glue after threshold filtering. *B,* Intensity ratio of the two functions shown in panel *A.*

Mean pressure drop across the rete and percent reduction in outflow following embolization for the various glue mixture groups (Lipiodol/NBCA ratio + GAA (μL)

Glue Mixture	ΔPressure (mm Hg)	% Flow Reduction	No. of Chronic/ No. of Acute Studies
50/50 + 20	17.6 ± 6.7	60.9 ± 18.1	1/5
50/50 + 10	17.3 ± 4.2	56.1 ± 9.4	1/5
50/50 + 5	15.0 ± 4.9	42.5 ± 13.9	1/5
50/50 + 0	16.0 ± 5.0	61.2 ± 16.2	1/5
80/20 + 0	20.78 ± 2.6	54.2 ± 8.7	3/3
P value	.93	.85	NA

pared by using a nonparametric ANOVA test (Kruskal-Wallis test).

Results

Effect of Lipiodol and Glacial Acetic Acid on NBCA Dispersion

The pressure drop across the rete and the flow reduction through the rete following embolization are summarized in Table 1. Although variations in flow reduction among the various embolic mixtures were statistically insignificant, a trend was observed. Better flow reduction was seen with increased amount of GAA in the Lipiodol/NBCA mixture. An erroneously higher flow reduction for the 50/50 + 0 (Lipiodol/NBCA + GAA) glue mixture may be attributed to a failure to collect (for unknown reasons) any blood from the draining cannula, which served as a venous outflow, in two acute AVM models after embolization; however, conventional radiographs of both retia showed a proximal and partial occlusion, whereas major parts of the rete remained patent (eg, Fig 4). Thus, significant residual flow through collateral meningeal branches can be expected. Although statistically insignificant, a higher mean pressure gradient was found across the rete after embolization by using the 80/20 + 0 glue mixture. This was related to higher number of chronic AVM models used in this subgroup ($n = 3$), with larger pressure gradients and flow before embolization compared with the acute AVM model (10).

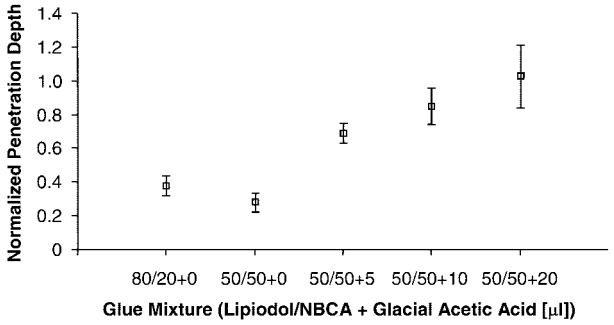

FIG 6. Penetration depth (mean values) for different glue mixtures in acute and chronic AVM model in swine (error bars denote the standard error of the mean [SEM]; $P = .002$).

Penetration depth into the rete for various glue mixtures is shown in Fig 6. Because the SDs were not comparable between the various groups, ANOVA by using the Kruskal-Wallis test was employed. The variations in penetration depth medians of the mixtures studied were found to be significant ($P = .002$). The mean penetration depth did not change significantly when the ratio of Lipiodol to NBCA in the mixture was reduced from 80% to 50%, despite reduction of mixture viscosity and presumed polymerization time due to smaller amounts of Lipiodol in the mixture; however, the addition of GAA to the 50/50 mixtures did increase the penetration depth. In a few cases, for mixtures containing 20 μL of GAA, the glue penetrated the entire rete, including the contralateral APA, which represented the draining vein of the AVM.

The average dispersion parameter indicating the spread of the various acrylate mixtures into smaller vessels is shown in Fig 7. Mixture dispersion was evaluated by using the same statistical analysis used for the penetration depth. Variations in increased dispersion with increased amount of GAA were found to be significant among the subgroups ($P = .022$).

Effect of Glue Mixture and GAA on Injection Force

The mean injection force and the impulse required to deliver the embolic mixture are shown in Fig 8 and

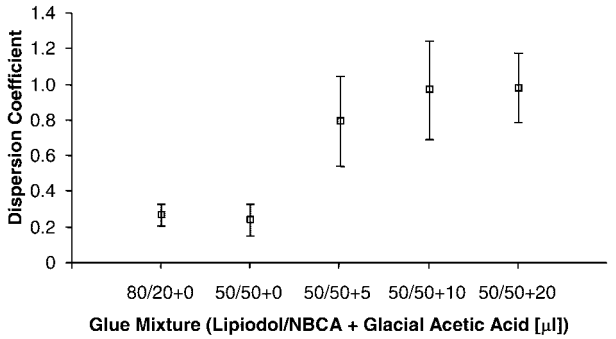

FIG 7. Mean of dispersion parameter for different glue mixtures in acute and chronic AVM model in swine (error bars denote SEM; $P = .022$).

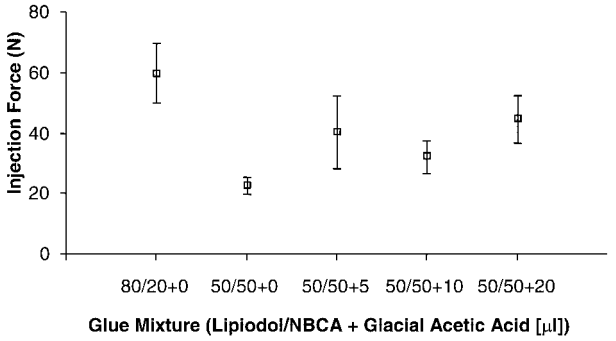

FIG 8. Used injection force (mean values) for different glue mixtures. Note one data set is excluded from 50/50 + 20 group. (Error bars denote SEM; $P = .044$).

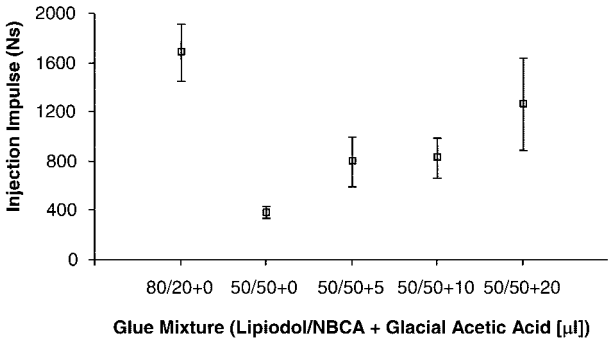

FIG 9. Injection impulse (mean values) for different glue mixtures. Note one data set is excluded from 50/50 + 20 group. (Error bars denote SEM; $P = .0023$).

Fig 9, respectively. Figure 8 shows that a higher force was needed to inject the 80/20 glue mixtures. The mean injection force for the 50/50 + 0 glue mixture was lower than the force needed to deliver glue mixtures containing GAA. Because the addition of GAA does not increase viscosity, the only explanation for the lower injection force used with the 50/50 + 0 glue mixtures may be attributed to the manual injection process. ANOVA assessment of variations in the mean injection force among the subgroups gave a P value of approximately 0.04. No significant linear trend was observed in the mean injection force as a function of GAA content in the glue mixture. Both Tukey-Kramer and Bonferroni posttest analyses found a statistically significant difference only between the higher (80/20) and lower (50/50) viscosity mixtures.

Mean injection impulse values were higher for the 80/20 mixtures than for 50/50 mixtures (Fig 9). Depending on the amount added, GAA prolonged the injection time of 50/50 glue mixtures, resulting in increased injection impulse. The impulse for the 50/50 + 0 glue mixture was the lowest, because short polymerization time prevented a long injection period. High impulse values with increasing amounts of GAA, however, resulted from a longer injection period and not necessarily a higher force of injection. The P value of the nonparametric test that assessed the variation in median injection impulse among the various subgroups was approximately 0.002. Dunn's multiple comparisons test showed a statistically significant difference only between the 80/20 and 50/50 + 0 subgroups.

Discussion

Two AVM models were constructed and used for NBCA embolization. The acute model is simple to construct, and its main purpose is to create an inexpensive reproducible model to test various embolization mixtures for penetration and dispersion. The chronic model is easy to construct, though the time elapsed between model creation and embolization is considerable, which makes this model expensive but allows evaluation of the embolizing agents in larger intranidal vessels.

In this study, we explored the effect of Lipiodol concentration in the glue mixture on penetration and dispersion by comparing the means of the penetration depths and dispersion parameters for two standard glue mixtures used in the clinical setting (ie, 80/20 and 50/50). The means were compared by using an unpaired t test. The difference in penetration depths was statistically insignificant ($P = .24$). The difference in dispersion parameters between the two groups was not significant either ($P = .79$). Therefore, we hypothesize that the addition of Lipiodol, after a certain amount, does not affect either the penetration depth or the dispersion of the glue mixture in plexiform AVMs with small diameter pedicles, as in the swine rete used for this study. One explanation for the limited contribution of Lipiodol can be its higher viscosity, compared with the viscosity of NBCA in the monomeric state. The higher viscosity mixture seems to hinder penetration and dispersion of the glue into small vessels before the completion of the polymerization process. Brothers et al (12) support this hypothesis in their study, which concluded that the addition of iophendylate oil would not effectively prolong polymerization time. In a more recent in vivo study, it was demonstrated that the Lipiodol concentration in the glue mixture has no significant effect on embolization kinetics (13).

For the chronic AVM models we used 1.2 mL NBCA and 1.2 mL Lipiodol to generate a 50/50 mixture. The concentration of GAA in the Lipiodol/acrylate mixture after adding 5, 10, and 20 μL was

0.21%, 0.42%, and 0.83% by volume, respectively; however, because the retia in the acute experiments were smaller in size, we mixed a volume of only 0.45 mL Lipiodol and 0.45 mL NBCA to create the 50/50 ratio mixtures. Thus, the concentration of GAA by adding 5, 10, and 20 μL to these mixtures was 0.28%, 0.55%, and 1.1% by volume, respectively. Although there is a discrepancy in the concentration of GAA used in the chronic and the acute experiments, we believe that the difference is too small to generate a substantial error between the two models. In an earlier study (13), we found that a 100% increase in GAA volume (from 10 μL to 20 μL) added to the same amount of embolic mixture resulted in a 25% increase in embolization time. In this study, the percent difference in the volume of GAA between the two models ranged from about 23.5% to 25.0%. Thus, it is reasonable to assume that this difference will introduce only a small change in the embolization time and consequently will have little effect on the penetration and dispersion of the embolic mixture.

Advances in microcatheter technology facilitate access to AVMs with small feeding arteries. A glue mixture of low initial viscosity allows a more controlled injection through a small-caliber microcatheter. Because the viscosity of poppy-seed oil is higher than NBCA, it is crucial to maintain its proportion as low as possible in the mixture. In our experience, a ratio of 50% oil by volume is the minimum required for visualization of the acrylate mixture under fluoroscopy. Deeper penetration and better dispersion of the embolic mixture should be achieved by proper addition of GAA. Numerous studies support this notion by showing that the addition of GAA resulted in a better control of polymerization (12–14).

The addition of 20 μL of GAA to the glue mixture in our study resulted, in a few cases, in penetration of the glue into the draining vein. This was a particular concern in the acute cases where the overall volume of the rete was smaller than in the chronic AVM cases and the ratio of GAA to oil/glue mixture was slightly higher. It is important to adjust the amount of GAA based on the volume and morphology of the AVM because it can be the decisive factor in the penetration depth of the glue mixture into the pathology.

It is noteworthy to stress that the notion of "plugging" an AVM to eliminate the pathology from the circulation is not sufficient. The benign inflammatory response and induced hyperplasia due to the embolic mixture result in permanent exclusion of the diseased vessels.

Conclusion

The viscosity of the liquid embolic agent used is an important limiting factor for embolization of an AVM. Decreasing the amount of Lipiodol improves nidus penetration. Quicker polymerization can be overcome by adding GAA that reduces the pH of the mixture. The addition of GAA to the Lipiodol/NBCA mixture produces a more homogenous distribution, with deeper penetration of the mixture. The acid also enhances the homogeneity of the dispersed glue mixture within the rete. Injection force is dependent on NBCA mixture to a lesser degree. On the basis of our study, a computer-controlled, rather than a manual injection, of embolic material seems feasible. This can be accomplished by using a microelectromechanical injector system with a pressure-sensitive and imaging feedback mechanism.

Appendix

A mathematical function consisting of four parameters was developed to model the penetration depth and the dispersion of the glue in the rete.

$$\text{A1)} \quad y = \begin{cases} A[(1\text{-}e^{\lambda*(l/l_g{}^{-1})})] & 0 \le l \le l_g \\ 0 & l_g < l \le l_{max} \end{cases}.$$

Here l_{max} is the rete total length, l_g is the penetration depth of the glue and A is the amplitude of the glue-penetration function. The dimensionless dispersion parameter, D, is obtained through scaling of the exponential factor λ by the cumulative grayscale intensity of the rete at the maximum glue penetration depth, i_r.

$$\text{A2)} \quad \lambda = (D * i_r)^{-1}.$$

The parameters of the mathematical model are determined by a constrained optimization process, which minimizes the sum of squares of the error between the data and the predicted values.

The constraints imposed on the range of the parameters are as follows (15):

- The magnitude of the model is restricted to the interval (0, 1).
- The centerline coordinate, l, is restricted to the maximum length of the centerline, l_{max}.
- The upper bound for λ is determined from the sampling interval, and the assumption that glue arrest cannot occur within one spatial sampling interval. To find the upper bound of λ, the function of equation (A1) needs to be evaluated at l_g and $l_{g\text{-}\Delta l}$.

$$\text{A3)} \quad y_{lg} = A[(1\text{-}e^{\lambda*(l_g/l_g{}^{-1})})] = 0$$

$$\text{A4)} \quad y_{lg\text{-}\Delta l} = A(l\text{-}e^{\lambda*[(l_g-\Delta l)/I_g-1]}).$$

The difference of the above equations, Δy, yields an expression for the upper bound of λ as:

$$\text{A5)} \quad \lambda_{max} = -\frac{l_g}{\Delta l}\ln\left(1-\frac{\Delta y}{A}\right).$$

Restricting the change in the glue penetration function per one sample interval, Δy, to be 90% of the total change in the amplitude of the glue penetration function, λ_{max} can be calculated as:

$$\text{A6)} \quad \lambda_{max} = 2.3\,\frac{l_g}{\Delta l}.$$

Therefore, for each rete we can set a constraint on the upper bound of λ that depends on the glue penetration depth and the sampling interval.

Although the physical interpretation of the amplitude of the function and the glue penetration depth is straightforward, the remaining two parameters require more careful examination. After the first bifurcation of the APA, successive branching of the vascular network occurs rapidly on each side of the rete, but it diminishes toward the interconnection of the two sides. When viewing the rete as an AVM model and crossing it from one APA to the other, a sharp increase in the number of vessels occurs followed by a decrease toward the midline and yet another increase past the midline and finally a rapid decrease until all the vessels coalesce into the contralateral APA. The vascular structure described above is neither monotonically increasing nor homogeneously distributed. Therefore, the dispersion of the glue depends on the location of its arrest in the rete. The simplest way to express the dependence of the dispersion on local morphology is to scale the dispersion parameter by the normalized value of the cumulative grayscale intensity of the rete at the location of the glue leading edge (i_r).

The normalized penetration depth, L, is calculated by using the following equation.

$$L = \frac{\left(l_g - l_{midline} + \frac{rete\ length}{2}\right)}{mean\ rete\ length}. \quad \text{A7)}$$

The average force during glue injection is calculated from the measured injection pressure, the known dimensions of the syringe, and the duration of the injection.

$$\bar{F} = \frac{\pi D^2}{4} \frac{1}{(t_f - t_i)} \int_{t_i}^{t_f} p(t)dt. \quad \text{A8)}$$

Here D is the syringe inner diameter, t_i is the time at the beginning of the injection, t_f is the time at the end of the injection, and $p(t)$ is the recorded pressure. The injection impulse is calculated as the product of the average force and the duration of the injection ($t_f - t_i$). The start- and endpoints of the injection are determined to be where the pressure exceeded 0.1 atmospheres and subsides to 0.1 atmospheres above atmospheric pressure. These threshold values represent about 2% of the maximum pressure during glue injection.

Acknowledgments

We gratefully acknowledge the financial support of the John R. Oshei Foundation and Toshiba America Medical Systems. We would like to thank the people of the Toshiba Stroke Research Center (State University of New York, Buffalo), led by Dr. L. N. Hopkins, where this work was completed, for their helpful support. We specifically acknowledge Dr. A. A Divani, who documented many aspects of this work in his dissertation that is referenced herein; Dr. M. Duffy-Fronckowiak, for her contribution to the statistical analysis; and Joseph Wodenscheck, who designed and built the data acquisition system. Moreover, we are grateful to Jason Kopko and Veronica Livescu, for their assistance during various parts of the experimental work.

References

1. Debrun GM, Aletich V, Ausman JI, et al. **Embolization of the nidus of brain arteriovenous malformations with N-butyl cyanoacrylate**. *Neurosurgery* 1997;40:112–120
2. DeMeritt JS, Pile-Spellman J, Mast H, et al. **Outcome analysis of preoperative embolization with N-butyl cyanoacrylate in cerebral arteriovenous malformations.** *AJNR Am J Neuroradiol* 1995;16:1801–1807
3. Fournier D, terBrugge KG, Willinsky R, et al. **Endovascular treatment of intracerebral arteriovenous malformations: experience in 49 cases.** *J Neurosurg* 1991;75:228–233
4. Wikholm G. **Occlusion of cerebral arteriovenous malformations with N-butyl cyano-acrylate is permanent.** *AJNR Am J Neuroradiol* 1995;16:479–482
5. Wikholm G, Lundqvist C, Svendsen P. **Embolization of cerebral arteriovenous malformations. Part I. Technique, morphology, and complications.** *Neurosurgery* 1996;39:448–457
6. Fournier D, terBrugge KG, Rodesch G, Lasjaunias P. **Revascularization of brain arteriovenous malformations after embolization with bucrylate.** *Neuroradiology* 1990;32:497–501
7. Gruber A, Mazal PR, Bavinzski G, et al. **Repermeation of partially embolized cerebral arteriovenous malformations: a clinical, radiologic, and histologic study.** *AJNR Am J Neuroradiol* 1996;17:1323–1331
8. Debrun GM, Viñuela F, Fox A, Drake CG. **Embolization of cerebral arteriovenous malformations with bucrylate.** *J Neurosurg* 1982;56:615–627
9. Pelz DM, Lownie SP, Fox AJ, Hutton LC. **Symptomatic pulmonary complications from liquid acrylate embolization of brain arteriovenous malformations.** *AJNR Am J Neuroradiol* 1995;16:19–26
10. Wakhloo AK, Lieber BB, Siekmann R, et al. **Acute and chronic swine rete arteriovenous malformation models: hemodynamics and vascular remodeling.** *AJNR Am J Neuroradiol* 2005;26:1702–1706
11. Siekmann R, Wakhloo AK, Lieber BB, et al. **Modification of a previously described arteriovenous malformation model in the swine: endovascular and combined surgical/endovascular construction and hemodynamics.** *AJNR Am J Neuroradiol* 2000;21:1722–1725
12. Brothers MF, Kaufmann JCE, Fox AJ, Deveikis JP. **N-butyl 2-cyanoacrylate: substitute for IBCA in interventional neuroradiology: histopathologic and polymerization time studies.** *AJNR Am J Neuroradiol* 1989;10:777–786
13. Gounis MJ, Lieber BB, Wakhloo AK, et al. **The effect of glacial acetic acid and ethiodized oil concentration on embolization using N-butyl 2-cyanoacrylate: an in vivo investigation.** *AJNR Am J Neuroradiol* 2002;23:938–944
14. Spiegel SM, Viñuela F, Goldwasser JM, et al. **Adjusting the polymerization time of isobutyl-2 cyanoacrylate.** *AJNR Am J Neuroradiol* 1986;7:109–112
15. Divani AA. *The distribution of various N-butyl 2-cyanoacrylate–based embolic mixtures in a swine rete model of arteriovenous malformations.* PhD dissertation, State University of New York at Buffalo, 2001